Exciton Formation in Semiconductors and the Influence of a Photonic Environment

M. Kira,[1] W. Hoyer,[2] T. Stroucken,[2] and S. W. Koch[2]

[1]*Laser Physics and Quantum Optics, Royal Institute of Technology, Lindstedsvägen 24, S-10044 Stockholm, Sweden*
[2]*Department of Physics and Material Sciences Center, Philipps University, Renthof 5, D-35032 Marburg, Germany*

(Received 6 April 2001; published 3 October 2001)

A fully microscopic theory is presented for interacting electrons, holes, photons, and phonons in semiconductor heterostructures. The formation dynamics and statistics of incoherent excitons are analyzed for different densities, lattice temperatures, and photonic environments. Luminescence experiments are shown to depend strongly on the photonic environment in contrast to suggested terahertz absorption measurements. Whereas luminescence in free space is dominated by plasma contributions, terahertz absorption should be able to directly measure excitonic populations.

DOI: 10.1103/PhysRevLett.87.176401 PACS numbers: 71.35.Lk, 42.70.Qs, 71.10.Pm

After the creation of electron-hole pairs, spontaneous recombination determines their ultimate lifetime even in ideal semiconductors. In this context, it is an old but still open question whether and under which conditions a significant population of incoherent bound excitons can form in such a nonequilibrium system where the ratio between bound and unbound pairs depends on the characteristic time scales of the relevant interaction processes. It is not even clear *a priori* how to count bound states since a rigorous exciton number operator does not exist [1]. However, one wants to understand the quantum statistical properties of these excitons, their distribution function, possible bosonic as well as Bose condensation aspects [2], and find ways to manipulate the exciton formation, e.g., with a photonic environment [3]. Furthermore, it is essential to know how to detect exciton populations experimentally.

In this Letter, we outline and evaluate a microscopic theory which is capable of solving the central problems discussed above. We include photon-, phonon-, and Coulomb-interaction effects microscopically and describe electrons, holes, and the possible exciton populations consistently in the Fermionic electron-hole picture. As a result, we are able to evaluate the excitonic correlations, formation rates, distribution functions, etc. for different temperatures and carrier densities without neglecting the underlying Fermionic antisymmetry. We show that the excitation of an incoherent system with a terahertz (THz) field yields an exact analog to atomic optics, thus identifying an exciton number in the atomic sense without the need of a number operator. This number is used to determine experimentally relevant conditions leading to incoherent exciton populations. A possibility to manipulate exciton distributions is studied using photonic band-gap structures [3]. To analyze the experimental possibilities for the detection of excitonic correlations, we compare photoluminescence to THz absorption and show that the THz signal can serve as an excellent measure for incoherent exciton populations, whereas luminescence always contains a fundamental plasma contribution which becomes dominant in many situations.

In the incoherent regime, the relevant two-point quantities are given by electron $f_k^{\mathrm{e}} = \langle e_k^\dagger e_k \rangle$ and hole $f_k^{\mathrm{h}} = \langle h_k^\dagger h_k \rangle$ occupations. Using the standard many-body Hamiltonian [4], f_k^{e} and f_k^{h} couple to four-point correlations $c_{\mathrm{e}}^{q,k',k} \equiv \delta\langle e_k^\dagger e_{k'}^\dagger e_{k'+q} e_{k-q} \rangle$, $c_{\mathrm{X}}^{q,k',k} \equiv \delta\langle e_k^\dagger h_{q-k}^\dagger h_{-k'} e_{k'+q} \rangle$, and $c_{\mathrm{h}}^{q,k',k} \equiv \delta\langle h_k h_{k'} h_{k'+q}^\dagger h_{k-q}^\dagger \rangle$, where $\delta\langle \hat{O} \rangle \equiv \langle \hat{O} \rangle - \langle \hat{O} \rangle_{\mathrm{HF}}$ denotes the correlations beyond the Hartree-Fock contributions $\langle \hat{O} \rangle_{\mathrm{HF}}$. To deal with the infinite hierarchy of correlations, we use a systematic truncation approach [5], which allows us to describe correlation effects at the desired level under all excitation conditions. Since we want to include all four-point correlations, we apply this method at the six-point level and obtain coupled equations,

$$\frac{\partial}{\partial t} f^{\mathrm{e(h)}} = \frac{2}{\hbar} \mathrm{Re}(V[c_{\mathrm{e(h)}}, c_{\mathrm{X}}] + \Gamma^{\mathrm{e(h)}} + R^{\mathrm{e(h)}}), \quad (1)$$

$$i\hbar \frac{\partial}{\partial t} c_{\mathrm{X}} = E_{\mathrm{X}} c_{\mathrm{X}} - i\Gamma[c_{\mathrm{X}}] + S_{\mathrm{X}} + U_{\mathrm{X}}[c_\lambda] + R_{\mathrm{X}}, \quad (2)$$

and the equivalent dynamics for $c_{\mathrm{e(h)}}$. These equations are written schematically and the brackets $[\ldots]$ denote a functional dependence. For example, the carrier densities are coupled to the four-point correlations via the Coulomb matrix-element V_k, they are cooled by phonons Γ_k^{e}, and depleted via the spontaneous emission contribution R_k^{e}. For the exciton correlations, $E_{\mathrm{X}}^{q,k',k}$ is the renormalized kinetic energy of two electron-hole pairs in $c_{\mathrm{X}}^{q,k',k}$. These four particles can interact via the two-body Coulomb interaction in six different ways which are described by $U_{\mathrm{X}}^{q,k',k}$ containing sums of the form $(1 - f_k^{\mathrm{e}} - f_{k-q}^{\mathrm{h}}) \sum_l V_{l-q} c_{\mathrm{X}}^{q,k',l}$. The phonon interaction is included microscopically in the terms $\Gamma^{q,k',k}$. Using the bath approximation [4] for phonons, Γ leads to phonon scattering induced dephasing such that no phenomenological dephasing is introduced. The quantity

$$S_{\mathrm{X}}^{q,k',k} = V_{k'+q-k}[\bar{f}_k^{\mathrm{e}} \bar{f}_{k-q}^{\mathrm{h}} f_{k'+q}^{\mathrm{e}} f_{k'}^{\mathrm{h}} - f_k^{\mathrm{e}} f_{k-q}^{\mathrm{h}} \bar{f}_{k'+q}^{\mathrm{e}} \bar{f}_{k'}^{\mathrm{h}}],$$

with $\bar{f}_k^\lambda = 1 - f_k^\lambda$, represents the Coulomb scattering of two uncorrelated electron-hole pairs. When only E_{X}, dephasing, and S_{X} are included, a scattering result at the level

of the second Born approximation is found [6], which describes equilibration of carrier densities via carrier-carrier scattering.

For the formation of excitons, the term S_X acts as a source, U_X enables bound states, and Γ provides scattering toward these states. In addition, the spontaneous emission recombines the densities and correlations via $R^{e(h)}$ and R_X which result from a photon emission $b_q^\dagger$ accompanied by a recombination of an electron-hole pair, i.e., $\langle b_q^\dagger h_{q-k} e_k \rangle$. This gives rise to luminescence into all directions and couples carriers and correlations into the semiconductor luminescence equations [7]. Polariton effects are included via the back coupling of the carrier dynamics to the light modes. In general, the spontaneous emission rates $R^{e(h)}$ and R_X are determined by the overlap-matrix elements of the confined carriers and the optical modes. Consequently, they depend on the local photonic density of states which in photonic crystals can exhibit large pseudogaps even if the total photonic density of states does not have a complete gap. Thus, a significant reduction of the radiative decay rates can be obtained by placing the semiconductor heterostructure in an antinode of the optical field inside a photonic crystal. In our calculations, we assume a reduction of the radiative decay rates by a factor of 100, which can already be achieved in present day samples [3].

The semiconductor luminescence equations together with Eqs. (1) and (2) and the dynamics of $c_{e(h)}$ form a closed set applicable to heterostructures of various dimensionality. Because of the overwhelming number of index combinations that has to be included, we restrict our numerical evaluation to an effectively one-dimensional model system, a quantum wire, where the carrier momenta are no longer vectors [8]. Nevertheless, we regard the numerical results presented below to be valid not only for quantum wires but qualitatively also for quantum wells [9].

We use the standard GaAs type parameters with a 3D-Bohr radius of $a_0 = 12.4$ nm and choose the corresponding wire confinement such that the lowest exciton state is 11 meV below the unrenormalized band edge in agreement with experiments [10]. The initial conditions of the computations correspond to the situation after an idealized incoherent excitation where both the electrical field and the interband polarization are vanishing and no correlations exist. For low enough temperatures, the exciton formation is eventually due to acoustic phonons [11]; only those are included in the analysis.

An intuitive picture of the exciton formation suggests that excitonic binding manifests itself as an increased probability to find electrons and holes close to each other. Therefore, we investigate the pair-correlation function $g(r) \equiv \langle \hat{n}^e(r) \hat{n}^h(0) \rangle$ which determines the conditional probability to find the electron density $\hat{n}^e(r)$ when the hole is located at $r = 0$ [12]. In the incoherent regime, the Hartree-Fock approximation leads to a constant $g^{HF}(r) = \langle \hat{n}^e(r) \rangle \langle \hat{n}^h(0) \rangle = n_0^2$, where n_0 is the spatially homogeneous carrier density. Thus, the genuine r dependence is always related to the correlated part; its explicit form is given by $\delta g(r) = \frac{1}{\mathcal{L}^2} \sum_{k,k',q} c_X^{q,k',k} e^{i(k'+q-k)r}$, with the normalization length $\mathcal{L}$. The inset of Fig. 1 shows the time evolution of $\delta g(r)$ when the system is initialized as an incoherent plasma with vanishing $\delta g(r)$. In order to have conditions favorable for exciton formation, low 10 K temperature and $na_0 = 0.03$ carrier density are used together with the photonic band-gap parameters. The pair-correlation function (solid lines) peaks at $r = 0$ and increases linearly in time after 300 ps. For comparison, the dashed line shows the $1s$-exciton probability $|\phi_{1s}(r)|^2$. The pair-correlation clearly has a similar shape, which is a direct evidence that exciton formation is in progress.

In order to identify the excitons, we seek a precise connection between population correlations and atomlike bound states. Traditionally, the occupation in atomic states is probed with light matching the energy difference of the states, implying THz fields for excitons [13]. Here, we consider the THz excitation to be perpendicular to the quantum wire. The minimal substitution [14] leads to the typical $\hat{J} \cdot A(t)$ interaction, where $A(t)$ is the vector field of the THz probe and $\hat{J} = \sum_k (j_k^e e_k^\dagger e_k + j_k^h h_k^\dagger h_k)$ with the current-matrix elements $j_k^{e(h)}$ related to the THz polarization $\frac{\partial}{\partial t} \hat{P}_{THz} \equiv \hat{J}/\mathcal{L}$. For an optically incoherent system [15], the THz polarization obeys the exact equation,

$$\frac{\partial^2}{\partial t^2} \langle P_{THz} \rangle = \frac{2}{\mathcal{L}} \sum_{q,\lambda>\nu} \omega_{\nu,\lambda} J_{\nu,\lambda} \, \mathrm{Im}[\delta \langle B_{\nu,q}^\dagger B_{\lambda,q} \rangle], \quad (3)$$

which depends only on excitonic correlations $\delta \langle B_{\nu,q}^\dagger B_{\lambda,q} \rangle$. They are connected to $c_X^{q,k',k}$ via the operator transformation $B_{\nu,q}^\dagger = \sum_k \phi_\nu(k) e_{k_e}^\dagger h_{-k_h}^\dagger$, where ϕ_ν is the density-dependent exciton wave function, and $k_{e/h} = k \pm [(m_{e/h})/(m_e + m_h)]q$ have been defined [4]. In Eq. (3), $\hbar \omega_{\nu,\lambda}$ is the energy difference of two exciton states and

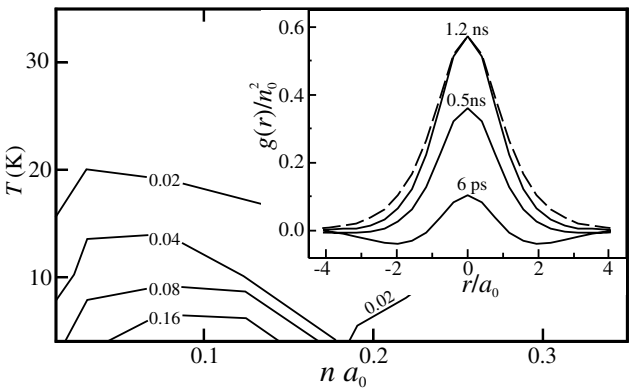

FIG. 1. Formation diagram for the lowest $1s$-exciton state as a function of density and temperature. Contour lines indicate constant relative formation rates $(\partial n_{1s}/\partial t)/n$ ranging from 0.02 to 0.16 ns^{-1}. The inset shows the pair-correlation function at 10 K and $na_0 = 0.03$ for different times after initialization of the system as uncorrelated electron-hole plasma. For comparison, the dashed line shows $|\phi_{1s}(r)|^2$ for the $1s$-exciton wave function.

$J_{\nu,\lambda} \equiv \sum_k \phi^\star_\nu(k)\,(j^e_k + j^h_k)\phi_\lambda(k)$ is the transition-matrix element between them, which leads to the ordinary selection rules equivalent to atoms. To determine $\langle P_{\mathrm{THz}}\rangle$, the dynamics of $\delta\langle B^\dagger_{\nu,q}B_{\lambda,q}\rangle$ have to be solved under influence of the THz probe and exciton formation dynamics. If the THz probe field is resonant with the lowest transition, we may limit the investigations to the first two excitons $\nu, \lambda = 1s, 2p$. By identifying quantities, $\langle S_-\rangle \equiv \sum_q \delta\langle B^\dagger_{1s,q}B_{2p,q}\rangle$, $\langle S_z\rangle \equiv \sum_q[\delta\langle B^\dagger_{2p,q}B_{2p,q}\rangle - \delta\langle B^\dagger_{1s,q}B_{1s,q}\rangle]/2$, $\langle S_x\rangle \equiv \mathrm{Re}[\langle S_-\rangle]$, $\langle S_y\rangle \equiv \mathrm{Im}[\langle S_-\rangle]$, $\mathbf{R} = (\langle S_x\rangle, \langle S_y\rangle, \langle S_z\rangle)$, and $\mathbf{\Omega} = (2J_{2p,1s}A(t), 0, \omega_{2p,1s})$, the Heisenberg equation of motion together with Eq. (2) leads to

$$\frac{\partial}{\partial t}\mathbf{R} = -\mathbf{\Omega} \times \mathbf{R} + \mathbf{R}_{\mathrm{deph}} + \delta\mathbf{R}_{\mathrm{Xform}} + \delta\mathbf{R}_{\mathrm{rec}}, \quad (4)$$

where $\mathbf{R}_{\mathrm{deph}}$ contains the dephasing due to phonons and $\delta\mathbf{R}$ terms include the exciton formation and spontaneous recombination of Eq. (2). When the THz probe is momentary compared to the exciton formation and recombination dynamics, $\delta\mathbf{R}$ terms can be neglected and we find the *terahertz Bloch equations* which have a one-to-one correspondence to the optical Bloch equations of atoms. This analogy can be used to compute the exciton number even though $B_{\nu,q}$ is not bosonic and $B^\dagger_{\nu,q}B_{\nu,q}$ is not a number operator, a problem which generally arises in many-body systems of composite bosons including atoms [1]. With the help of the identification provided by the Bloch vector $\mathbf{R}$, we can use $\delta N_\nu(q) \equiv \delta\langle B^\dagger_{\nu,q}B_{\nu,q}\rangle$ to determine the number of incoherent excitons in state ν.

To obtain an overview of the conditions which lead to a significant formation of excitons in our model system, we vary the lattice temperature from 4 to 70 K and the carrier density from $na_0 = 0.025$ to 0.375. We determine the linear formation rate of $1s$ excitons $\delta n_{1s} = \sum_q \delta N_{1s}(q)/\mathcal{L}$. Figure 1 summarizes the computed relative formation rates $r_f \equiv (\partial\delta n_{1s}/\partial t)/n$ in a temperature-density diagram. We observe strong formation only below 15 K and $na_0 = 0.18$. Above 30 K and $na_0 = 0.3$, the formation is negligible since it takes over 20 ns to convert 10% of the carrier density into bound excitons [16].

The effect of the radiative environment is studied directly in Fig. 2 by plotting the $1s$-exciton occupation $\delta N_{1s}(q)$ with the strong (dashed line) and weak (solid line) spontaneous emission for the same conditions as in the inset of Fig. 1. Both distributions show clear deviations from a thermal bosonic exciton distribution (dotted line). Since primarily excitons with relatively large momentum are formed, the exciton distribution shows a long tail even though the phonon scattering tends to thermalize the distributions. The thermalization also has to compete with spontaneous recombination, scattering to other exciton states, and effects due to the Fermion character. Since the photon momentum is negligible compared to the exciton momentum, mostly $q \approx 0$ excitons participate in recombination and luminescence. Thus, strong spontaneous emission leads to a significant hole burning in the excitonic distribution function around $q = 0$ since recombination depletes the correlations faster than they can build up. Still, the relative momentum of the recombining pairs is not restricted, such that f^{e} and f^{h} are depleted evenly.

To determine how the incoherent populations can be detected in a measurement, we compare photoluminescence to THz-absorption spectra. The inset of Fig. 2 shows the computed luminescence spectra with and without photonic inhibition. In free-space systems, exciton populations contribute only weakly to the $1s$ luminescence which is mainly determined by plasma contributions; i.e., Hartree-Fock luminescence dominates the full emission even if luminescence at the exciton energy is observed [17]. Only inside a photonic crystal, excitonic population can build up into small momentum states such that the correlated pairs dominate the emission. Even though the majority of excitons remains unchanged by the photonic environment, the luminescence spectrum drastically changes since all the dark excitons with nonvanishing center-of-mass momentum do not contribute. Also, other phenomena such as Bose-Einstein-like condensation require a significant population of small momentum states. This can be achieved only when the spontaneous emission is inhibited.

When a weak-probe solution of Eq. (4) is used in Eq. (3), we obtain the linear THz absorption [13],

$$\alpha_{\mathrm{THz}}(\omega) = \mathrm{Im}\left[\frac{|d_{12}|^2[\delta n_{1s} - \delta n_{2p}]}{\hbar\omega_{2p,1s} - \hbar\omega - i\gamma}\right], \quad (5)$$

with the dipole-matrix element $|d_{12}| = |J_{1s,2p}/\omega|$. Figure 3 shows the time evolution of the THz-absorption peak

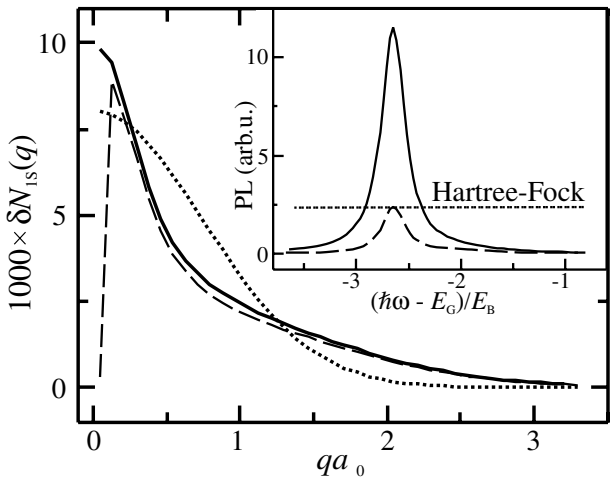

FIG. 2. Momentum distribution of the correlated $1s$ excitons after 1.1 ns at 10 K and $na_0 = 0.03$. The free-space (dashed line) and photonic band-gap (solid line) results are compared with a corresponding thermal distribution (dotted line). The inset shows the photoluminescence spectra (band-gap emission multiplied by 100 to compensate the reduced optical coupling) together with the peak height of the corresponding Hartree-Fock result. Energies are given relative to the unrenormalized band edge in units of the 3D-binding energy $E_B = 4.2$ meV.

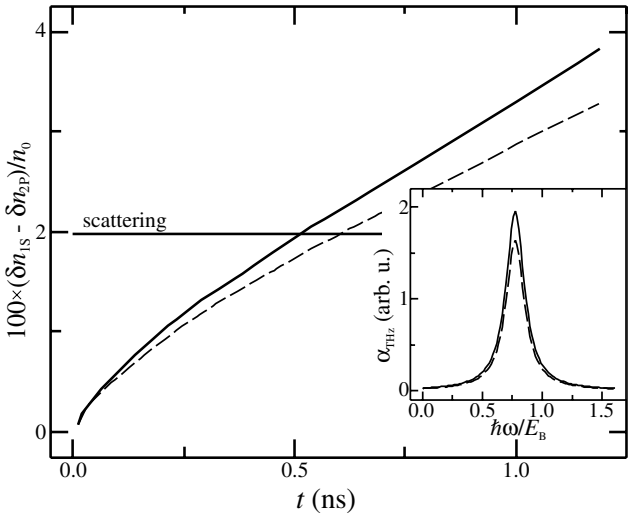

FIG. 3. The correlated THz-inversion factor is plotted for a free-space (dashed line) and a photonic band-gap (solid line) system as function of time at 10 K and $na_0 = 0.0125$. The corresponding second Born result is indicated by the horizontal line. The inset shows the THz-absorption spectrum at 1.1 ns.

height, $\delta n_{1s} - \delta n_{2p}$, in free space (dashed line) and in the photonic band-gap structure (solid line). The horizontal line indicates the corresponding second Born scattering result. The free-space and inhibited emission results are similar, increasing linearly beyond the scattering result due to exciton formation. In contrast to luminescence, THz absorption depends only on the correlated exciton populations and probes excitons with all momenta. As a result, THz absorption provides an unambiguous method, rather insensitive to the radiative environment, to determine incoherent exciton occupations.

In summary, our model analysis consistently treats free carriers, bound excitons, as well as their coupling to photons and phonons, and identifies conditions favorable for exciton formation. The stationary exciton population is governed by a balance between formation and radiative decay. As long as spontaneous emission is fully allowed, the pair states with small momentum are strongly depleted such that most excitons are in dark states and the luminescence signal is dominated by the free-carrier contributions. At the same time, the one-particle distributions are basically in quasiequilibrium. Inhibited spontaneous emission, as in optical band-gap structures, is required to significantly enhance the formation of excitons with small center-of-mass momentum. Irrespective of the photonic coupling of the excitonic dipole transition, terahertz absorption experiments can measure excitonic populations with any center-of-mass momentum.

This work was supported by the Deutsche Forschungsgemeinschaft through the photonic crystal and the Leibniz programs and by the Humboldt Foundation and Max-Planck Society through the Max-Planck Research program. M. K. thanks the Swedish Research Council (TFR and NFR), the Göran Gustafssons foundation, and the Center for Parallel Computers.

[1] T. Usui, Prog. Theor. Phys. **23**, 787 (1960); C. I. Ivanov, H. Barentzen, and M. D. Girardeau, Physica (Amsterdam) **140A**, 612 (1987).
[2] D. Snoke, J. P. Wolfe, and A. Mysyrowicz, Phys. Rev. Lett. **59**, 827 (1987); K. Johnson and G. M. Kavoulakis, *ibid.* **86**, 858 (2001).
[3] See, e.g., E. Yablonovitch, Phys. Rev. Lett. **58**, 2059 (1987); S. John, *ibid.* **58**, 2486 (1987); D. Labilloy *et al., ibid.* **79**, 4147 (1997).
[4] For a textbook discussion, see H. Haug and S. W. Koch, *Quantum Theory of the Optical and Electronic Properties of Semiconductors* (World Scientific, Singapore, 1994), 3rd ed.
[5] J. Fricke, Ann. Phys. (N.Y.) **252**, 479 (1996).
[6] F. Jahnke, M. Kira, and S. W. Koch, Z. Phys. B **104**, 559 (1997).
[7] M. Kira, W. Hoyer, F. Jahnke, and S. W. Koch, Prog. Quantum Electron. **23**, 189 (1999).
[8] F. Rossi and E. Molinari, Phys. Rev. Lett. **76**, 3642 (1996); F. Tassone and C. Piermarocchi, *ibid.* **82**, 853 (1999).
[9] In collaboration with Filinov, quantum Monte Carlo simulations (thermal equilibrium without photons) reproduced key results of our theory in that limit. These simulations were extended to two dimensions without changing the qualitative features of our main conclusions.
[10] R. Ambigapathy *et al.,* Phys. Rev. Lett. **78**, 3579 (1997); R. Kumar *et al., ibid.* **81**, 2578 (1998).
[11] A. Thränhardt *et al.,* Phys. Rev. B **62**, 2706 (2000).
[12] R. Zimmermann, *Many-Particle Theory of Highly Excited Semiconductors* (Teubner Verlagsgesellschaft, Leipzig, 1988), 1st ed.
[13] R. H. M. Groeneveld and D. Grischkowsky, J. Opt. Soc. Am. B **11**, 2502 (1994); J. Cêrne *et al.,* Phys. Rev. Lett. **77**, 1131 (1996).
[14] C. Cohen-Tannoudji, J. Dupont-Roc, and G. Grynberg, *Photons and Atoms* (Wiley, New York, 1989), 3rd ed.
[15] In contrast to the incoherent regime, coherent excitons lead to a THz signal which is dominated by the Hartree-Fock contribution; see, e.g., S. Hughes and D. S. Citrin, Opt. Lett. **24**, 1068 (1999).
[16] The single-particle carrier densities may remain unchanged even when two-particle populations are formed.
[17] M. Kira, F. Jahnke, and S. W. Koch, Phys. Rev. Lett. **81**, 3263 (1998).